

The Intracellular Distribution and Pattern of Expression of Mcl-1 Overlap with, but Are Not Identical to, Those of Bcl-2

Tao Yang,[‡] Karen M. Kozopas,[‡] and Ruth W. Craig^{*‡}

^{*}Department of Pharmacology and Toxicology, Dartmouth Medical School, Hanover, New Hampshire 03755-3835; and [‡]Department of Physiology, Johns Hopkins School of Medicine, Baltimore, Maryland 21205

Abstract. A family of genes related to the bcl-2 protooncogene has recently emerged. One member of this family, mcl-1, was cloned from a human myeloblastic leukemia cell line (ML-1) undergoing differentiation. The intracellular localization of mcl-1, as well as the kinetics of its expression during differentiation, have now been studied. These studies show that the intracellular distribution of mcl-1 overlaps with, but is not identical to, that of bcl-2: mcl-1 is similar to bcl-2 in that the mcl-1 protein has a prominent mitochondrial localization, and in that it associates with membranes through its carboxyl hydrophobic tail. mcl-1 differs from bcl-2, however, in its relative distribution among other (nonmitochondrial/heavy membrane) compart-

ments, mcl-1 also being abundant in the light membrane fraction of immature ML-1 cells while bcl-2 is abundant in the nuclear fraction. Similarly, in differentiating ML-1 cells, the timing of expression of mcl-1 overlaps with, but is not identical to, that of bcl-2: the mcl-1 protein increases rapidly as cells initiate differentiation, and mcl-1 is a labile protein. In contrast, bcl-2 decreases gradually as cells complete differentiation. Overall, the mcl-1 and bcl-2 proteins have some properties in common and others that are distinct. A burst of expression of mcl-1, prominently associated with mitochondria, complements the continued expression of bcl-2 in ML-1 cells differentiating along the monocyte/macrophage pathway.

MCL-1, a member of the bcl-2 family, was cloned from the ML-1 human myeloblastic leukemia cell line (26). ML-1 cells proliferate as immature myeloblasts, and they differentiate to monocytes and macrophages upon exposure to the phorbol ester, 12-O-tetradecanoylphorbol 13-acetate (TPA)¹ (9). The progression to differentiated phenotype is accompanied by a loss of proliferative capacity without substantial loss of viability. mcl-1 was isolated by screening for genes that increase in expression early in the switch from proliferative to differentiating phenotype (26).

It is the carboxyl portion of mcl-1 that has sequence similarity to bcl-2 (the carboxyl 139 out of the 350 amino acid residues of mcl-1 [25]; bcl-2 sequence [8, 52]). At the extreme carboxyl terminus, both mcl-1 and bcl-2 have a hydrophobic stretch (19–20 amino acids); in bcl-2, this stretch mediates the association of the protein with membranes (6, 7, 38, 51). bcl-2 was initially reported to localize to mitochondrial membranes and has since also been found in other intracellular membrane-containing compartments, including the nuclear envelope and endoplasmic reticulum (21, 27, 33). Recent data show that bcl-2 associates with the outer

mitochondrial membrane, and that it is targeted there by the hydrophobic carboxyl terminus (27, 35, 38).

Along with its remarkable intracellular distribution, bcl-2 has an interesting function, which is to inhibit cell death. This can be seen in cell lines dependent on growth factors, where exogenous introduction of bcl-2 inhibits the apoptosis produced by growth factor deprivation (16, 31, 39, 53). bcl-2 can similarly inhibit cell death caused by certain cytotoxic agents (23, 46, 48) or by apoptosis-inducing gene products such as c-myc (3, 14). The role of bcl-2 in inhibiting death is also seen in vivo: in mice lacking bcl-2, the lymphoid system appears normal at birth, but subsequently collapses because of apoptosis of lymphoid cells (36, 54). Conversely, mice expressing a transgenic bcl-2 exhibit enhanced survival of lymphoid cells (31, 48, 49, 50). Finally, the endogenous pattern of expression of bcl-2 reflects its role in the inhibition of apoptosis (22). For example, bcl-2 is not expressed in the majority of immature thymocytes (CD4⁺CD8⁺), which are susceptible to apoptotic death; however, bcl-2 is expressed in those cells that survive and continue to differentiate (17, 29, 55).

Like mcl-1, other genes in the bcl-2 family exhibit sequence relatedness in the carboxyl portion. Cellular genes in this family include bcl-x (4), bax (40), A1 (28), and ced-9 (20). Although the intracellular sites of action of many of these gene products have not yet been fully elucidated, it is known that most can influence cell death. Some, like mcl-1 and bcl-2, cause an enhancement of cell viability under

Address all correspondence to Dr. Ruth W. Craig, Department of Pharmacology and Toxicology, Dartmouth Medical School, Hanover, NH 03755-3835. Tel. (603) 650-1657. Fax: (603) 650-1129.

1. *Abbreviation used in this paper:* TPA, 12-O-tetradecanoylphorbol 13-acetate.

apoptosis-inducing conditions (4, 20, 42), while others (e.g., bax; reference 40) cause an inhibition. Two viral genes (BHRF1 [41] and LMW5 [37]) are distantly related to bcl-2. The BHRF1 gene product is membrane-associated, and it has recently been reported to inhibit cell death and to localize to mitochondria (19, 41). One aim of the research reported in this paper was to investigate the intracellular localization and membrane association of one of the cellular members of the bcl-2 family, mcl-1.

In contrast to the sequence relatedness in the carboxyl portion, mcl-1 differs from bcl-2 and other family members in its amino terminal portion. One difference is that the extreme amino terminus of mcl-1 has partial signal sequence character (26). Thus, as part of our studies on localization, we considered whether mcl-1 might be processed by the endoplasmic reticulum through a signal sequence-mediated mechanism. A second difference between mcl-1 and bcl-2 is that mcl-1 contains PEST sequences (26), which frequently signal rapid protein turnover (43). We thus measured the half-life of mcl-1 with the expectation that mcl-1 might be a labile protein. bcl-2 is a long-lived protein, having a half-life of 10–14 h (12, 24, 32). We also monitored the expression of mcl-1 and bcl-2 during TPA-induced ML-1 cell differentiation; this was to determine whether the patterns of expression of the two proteins were noncoordinate, as might be expected with differing stabilities.

In sum, we have examined the intracellular localization and kinetics of expression of the mcl-1 protein. Our findings show that in ML-1 cells initiating differentiation along the monocyte/macrophage pathway, continuous expression of bcl-2 is accompanied by a burst of expression of mcl-1, which is associated prominently with mitochondria. Overall, mcl-1 and bcl-2 exhibit overlapping, but nonidentical, intracellular distributions and patterns of expression.

Materials and Methods

Antibodies

We produced polyclonal antiserum to the mcl-1 protein as follows: a cDNA containing the entire coding region of mcl-1 (pIA6 [26]) was inserted into the pGEX-2T bacterial expression vector (Pharmacia Fine Chemicals, Piscataway, NJ), using the EcoRI restriction site. This construct was introduced into a protease-deficient (*lon*⁻) strain of *Escherichia coli*, SRP84, and expression of the mcl-1-GST fusion protein was induced by addition of 0.5 mM isopropyl- β -D-thio-galactopyranoside. After resuspension in MT-PBS buffer (150 mM NaCl, 16 mM Na₂HPO₄, 4 mM NaH₂PO₄, pH 7.3), bacteria were lysed using a French pressure cell press (three times at 18,000 psi). After centrifugation at 20,000 g, the mcl-1-GST fusion protein in the supernatant was purified by affinity chromatography on glutathione agarose (Sigma Immunochemicals, St. Louis, MO). On SDS-PAGE, the fusion protein was seen as a doublet (66–68 kD). The mcl-1 portion of the fusion protein could be released from the GST portion by cleavage with thrombin (Sigma). This yielded a band of 26.5 kD (the expected size for GST) and a doublet of 40–42 kD (approximately the expected size for mcl-1). The 42-kD component of this doublet was transferred to polyvinylidene difluoride membrane and subjected to NH₂-terminal sequencing using Edman degradation. 15 amino acid residues were sequenced and found to be exactly as expected: the first six residues derived from the polylinker, and the remaining nine were from the mcl-1 cDNA, with three of the latter deriving from 5' sequence that is not normally translated (26). The 42-kD band was therefore excised and used for immunization of two New Zealand white rabbits (JH746 and JH747). Immunizations were carried out by Hazelton Research Products Inc. (Denver, PA).

The SPA825 and SPA827 antibodies were purchased from StressGen Biotechnologies (Victoria, B.C., Canada). The H5C6 antibody to CD63 (Pltgp40, see reference 1) was provided by Dr. James Hildreth (Johns Hop-

kins School of Medicine, Baltimore, MD). The Ab1QA5 antibody was from Dr. Lanbo Chen (Dana-Farber Cancer Institute, Boston, MA).

Affinity Purification and Analysis of the Specificity of the Anti-mcl-1 Antibody

The ImmunoPure Ag/Ab immobilization kit (Pierce Chemical Co., Rockford, IL) was used for affinity purification, coupling of the mcl-1-GST fusion protein to the activated gel, and further steps, being carried out using the manufacturer's instructions.

The specificity of the anti-mcl-1 antiserum was tested in Western blots against the bacterially produced mcl-1-GST protein. SDS-PAGE was carried out using the mcl-1-GST fusion protein (before and after digestion with thrombin to yield mcl-1 and GST). The anti-mcl-1 antiserum detected mcl-1 before and after digestion of the fusion protein (Fig. 1 A, 66–68 kD fusion protein in lane 6 and 40–42 kD mcl-1 protein in lane 5). The smaller bands detected may represent partial degradation products. The large band detected in lane 5 probably represents uncleaved fusion protein. The antiserum did not detect GST (Fig. 1 A, lane 4). Preimmune serum did not detect mcl-1 (Fig. 1 A, lanes 1–3).

Specificity was also tested in Western blots against lysates of ML-1 cells. Lysates from both uninduced (*cont*) and TPA-induced cells were used, since the latter would be expected to express higher levels of mcl-1 (26). In cells induced with TPA for 3–4 h, the antiserum detected a doublet of 40–42 kD (Fig. 1 B, lane 8) that was not detected by preimmune serum (Fig. 1 B, lane 10). The affinity-purified antibody preparation also detected this doublet (Fig. 1 B, lane 6). The appearance of this doublet was blocked by previous addition of a fivefold excess of mcl-1-GST fusion protein to the antibody (Fig. 1 B, lane 2), but it was not blocked by addition of the same concentration of GST protein (Fig. 1 B, lane 4). These data show that our antibody preparations specifically detect mcl-1. This antibody does not exhibit cross-reactivity to bcl-2, which was detected as a single band of 26 kD (antibody from Dako Corp., Carpinteria, CA). The affinity-purified anti-mcl-1 antibody preparation was used in all further experiments, with the exception of immunoprecipitations, where the anti-mcl-1 antiserum was used. With immunoprecipitation, as with Western blotting (Fig. 1 B), the specific mcl-1 bands were well separated from nonspecific bands, as determined by using preimmune serum (see Figs. 4 A and 8).

Immunofluorescence Microscopy

Immunofluorescent staining of ML-1 cells was carried out after 3×10^4 cells were cytocentrifuged onto coverslips. Cells were fixed in 2% paraformaldehyde in PBS (15 min), washed with PBS, and blocked and permeabilized in PBS containing 2% goat serum, 0.1% saponin, and 0.02% Na₃ (15 min). Cells were then incubated for 1 h with affinity-purified mcl-1 antibody (5 μ g/ml in PBS containing 3% BSA). After three washes with PBS, cells were incubated for 1 h with fluorescein- or Texas red-conjugated goat anti-rabbit IgG antibody (10 μ g/ml; Jackson ImmunoResearch Laboratories, Inc., West Grove, PA). After three washes with PBS, cells were mounted and observed using conventional or confocal fluorescence microscopy. All the above steps were carried out at room temperature. Sequential confocal images (from a "Z series") were superimposed to produce a projection image when a fluorescent image was compared to its phase-contrast counterpart.

Two-color staining was carried out essentially as above, except for the addition of a second primary antibody. The secondary antibody to the second primary antibody was Texas red- or FITC-conjugated goat or sheep anti-mouse IgG antibody. Rhodamine123 was purchased from Molecular Probes, Inc. (Eugene, OR), and it was applied to cells at 10 μ g/ml for 30 min.

Subcellular Fractionation

For differential centrifugation, cells ($1-2 \times 10^8$) were collected by centrifugation, washed once with PBS and twice with hypotonic buffer (10 mM Hepes, pH 7.4, 42 mM KCl, and 5 mM MgCl₂), resuspended in 2 ml of hypotonic buffer containing protease inhibitors (1 mM PMSF, 0.1 mM EDTA, 0.1 mM EGTA, 1 mM DTT, 1 μ g/ml pepstatin A, 1 μ g/ml leupeptin, and 5 μ g/ml aprotinin), and lysed with a Dounce homogenizer. The total cell lysate (T) obtained was then centrifuged at 500 g for 5 min. The pellet was washed three times with 1.6 M sucrose and lysed in 0.5–1 ml Lysis buffer (50 mM Tris-Cl, pH 8.0, containing 1% NP-40, 0.1% SDS, 2 mM EDTA, and the above protease inhibitors), to yield the nuclear fraction (N). The supernatant was subjected to further centrifugation at 10,000 g for 30

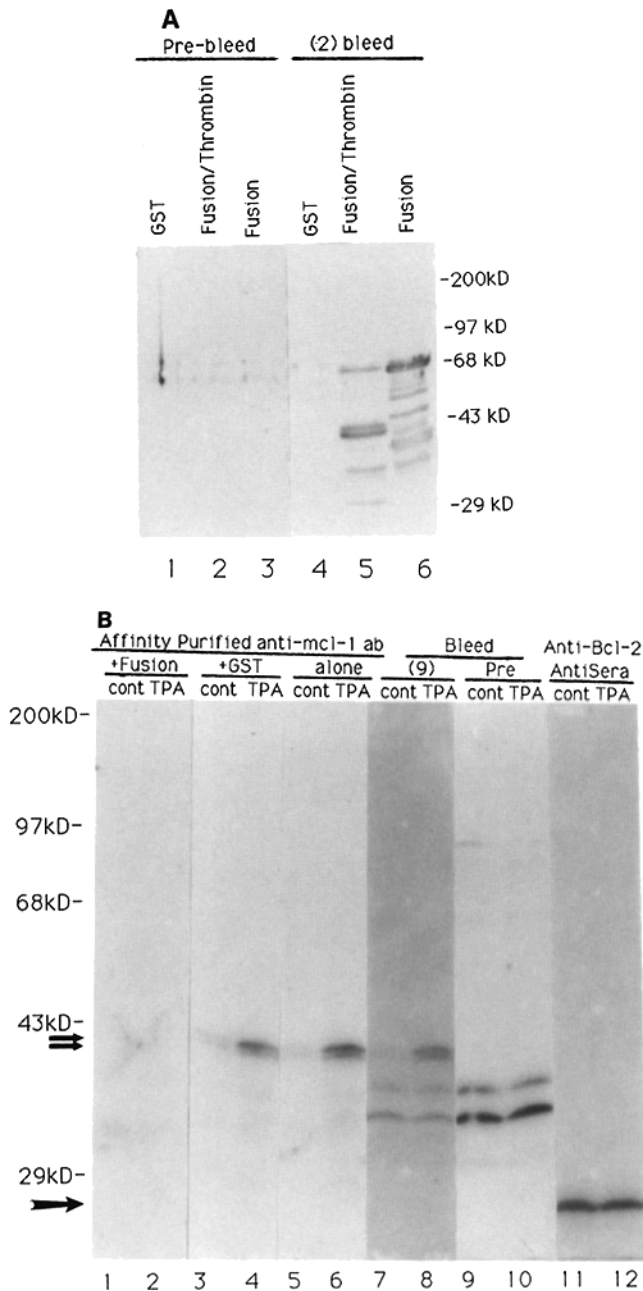


Figure 1. Specificity of the anti-mcl-1 antibody. (A) the mcl-1-GST fusion protein (*Fusion*, lanes 2, 3, 5, and 6), or GST itself (lanes 1 and 4) were produced by expression in *Escherichia coli*. These proteins were subjected to SDS-PAGE, with the mcl-1-GST fusion protein being used both before (lanes 3 and 6) and after (lanes 2 and 5) cleavage with thrombin (which cleaves the GST away from the mcl-1). Western blotting was carried out using either preimmune serum (lanes 1-3) or immune serum (*bleed* (2), lanes 4-6). (B) ML-1 cells were grown in the absence (*cont*) or presence of TPA (10^{-9} M for 3.75 h). Western blotting was carried out using lysate from the equivalent of 4×10^6 cells in each lane. Affinity-purified anti-mcl-1 antibody (lanes 1-6) was used either alone (lanes 5 and 6) or after preincubation with a fivefold excess of mcl-1-GST fusion protein (*Fusion*, lanes 1 and 2) or GST (lanes 3 and 4). The mcl-1 antiserum was also used without purification (*bleed* (9), lanes 7 and 8), along with preimmune serum from the same rabbit (lanes 9 and 10). Antiserum to bcl-2 is shown for comparative purposes (lanes 11 and 12). Double arrows indicate the upper

min. The resulting pellet was washed with 1 ml hypotonic buffer and lysed in lysis buffer to yield the heavy membrane fraction (H). The supernatant was subjected to centrifugation at 150,000 g for 1 h, with the final pellet being suspended in lysis buffer to yield the light membrane fraction (L), and the final supernatant yielding the cytosolic fraction (C).

To assess the membrane association of mcl-1, Triton X-114 fractionation and phase separation were carried out as described (5).

Transfection of mcl-1 into cos-1 Cells

mcl-1 cDNAs were inserted into the EcoRI site of an expression vector that uses the SV-40 early promoter (pSG5; Cloning Systems; Stratagene, La Jolla, CA). One construct, pSG5-mcl-1, was constructed to contain the entire mcl-1 coding region; this construct was derived by digesting pLA6 (26) with EcoRI and ligating the released mcl-1-containing fragment into pSG5. A second construct, pSG5-mcl-1 Δ C27, was constructed to lack the hydrophobic stretch at the carboxyl terminus, with the carboxyl 27 amino acids of mcl-1 being replaced by a stuffer fragment. pSG5-mcl-1 Δ C27 was derived as follows: first, a plasmid containing the mcl-1 coding region (plambda5) was partially digested with Eco0109 and DraII to remove a fragment that contains the carboxyl 27 amino acids (yielding plambda5 Δ Eco0109#5 [25], which contains nucleotide residues 33-1029 of the mcl-1 cDNA). The truncated mcl-1 from this plasmid was excised from Bluescript with EcoRI and BssHIII, and it was cloned into pSG5 by blunt end ligation; a stop codon present in pSG5 results in the formation of a protein that has the same molecular weight as wild-type mcl-1, but that lacks a hydrophobic domain at its carboxyl terminus (amino acid residues 1-323 of mcl-1 are followed by translated vector sequences, yielding a protein that has the same molecular weight as mcl-1, but that migrates slightly more slowly (see reference 2 and references therein). Using the DEAE-dextran method (45), these plasmids were transfected into cos-1 cells that had been grown to 30-50% confluence. After 24 h, these cells were assayed for membrane association of the mcl-1 protein, as described above.

Western Blotting

Western blotting was carried out using standard methods with minor modifications (11). Briefly, cells were washed twice with ice-cold PBS, lysed by resuspension in SDS sample buffer (62.5 mM Tris-Cl, pH 6.8, 2% SDS, 5% 2-mercaptoethanol, 10% glycerol, and 0.01% bromophenol blue), boiled for 5 min, and stored at -20°C . Cell lysates were subjected to SDS-PAGE (12%) and transferred to nitrocellulose membrane. The membranes were rinsed with PBS, blocked with 5% nonfat dry milk in PBS, washed with PBS, incubated for 2 h with the mcl-1 antibody (5 $\mu\text{g}/\text{ml}$ [in PBS containing 3% BSA and 0.02% NaN_3]), and washed with PBS. Detection used either ^{125}I -protein A or horseradish peroxidase-conjugated secondary antibodies (donkey anti-rabbit Ig or sheep anti-mouse Ig [Amersham Corp., Arlington Heights, IL] diluted at 1:1,000 in 2% horse or sheep serum), followed by incubation with enhanced chemiluminescence reagents. The above incubations and washes were carried out at room temperature.

Densitometric scanning was used to estimate relative amounts of the mcl-1 protein, using autoradiographs from several different exposure times and avoiding the use of overexposed autoradiographs. In scans of Western blots (see Figs. 5 and 6), the values used represent the total mcl-1 protein since the various forms of mcl-1 were not separated well enough to be quantitated individually. In Fig. 6, the fold increase in mcl-1 at various times after addition of TPA was calculated relative to the amount of mcl-1 present at time 0.

Metabolic Labeling and Immunoprecipitation

Metabolic labeling and immunoprecipitation were carried out using established methods (11). Cells were washed twice and suspended at 2.5×10^6 cells/ml, using methionine-free RPMI medium 1640 containing 7.5% dialyzed serum. (When a time point of 24 h was used, the medium consisted of this methionine-depleted medium [90%] plus standard methionine-containing medium [10%]). At various times after addition of L - ^{35}S -methionine (0.2 mCi/ml), 5×10^6 cells were washed twice with PBS and lysed in 50 mM Tris-Cl, pH 7.6, containing 150 mM NaCl, 1% bovine hemoglobin, 1% NP-40, 0.5% deoxycholate, 0.1% SDS, 2 mM EDTA, 1 mM

and middle mcl-1 protein bands apparent at early times (3-4 h) after exposure to TPA.

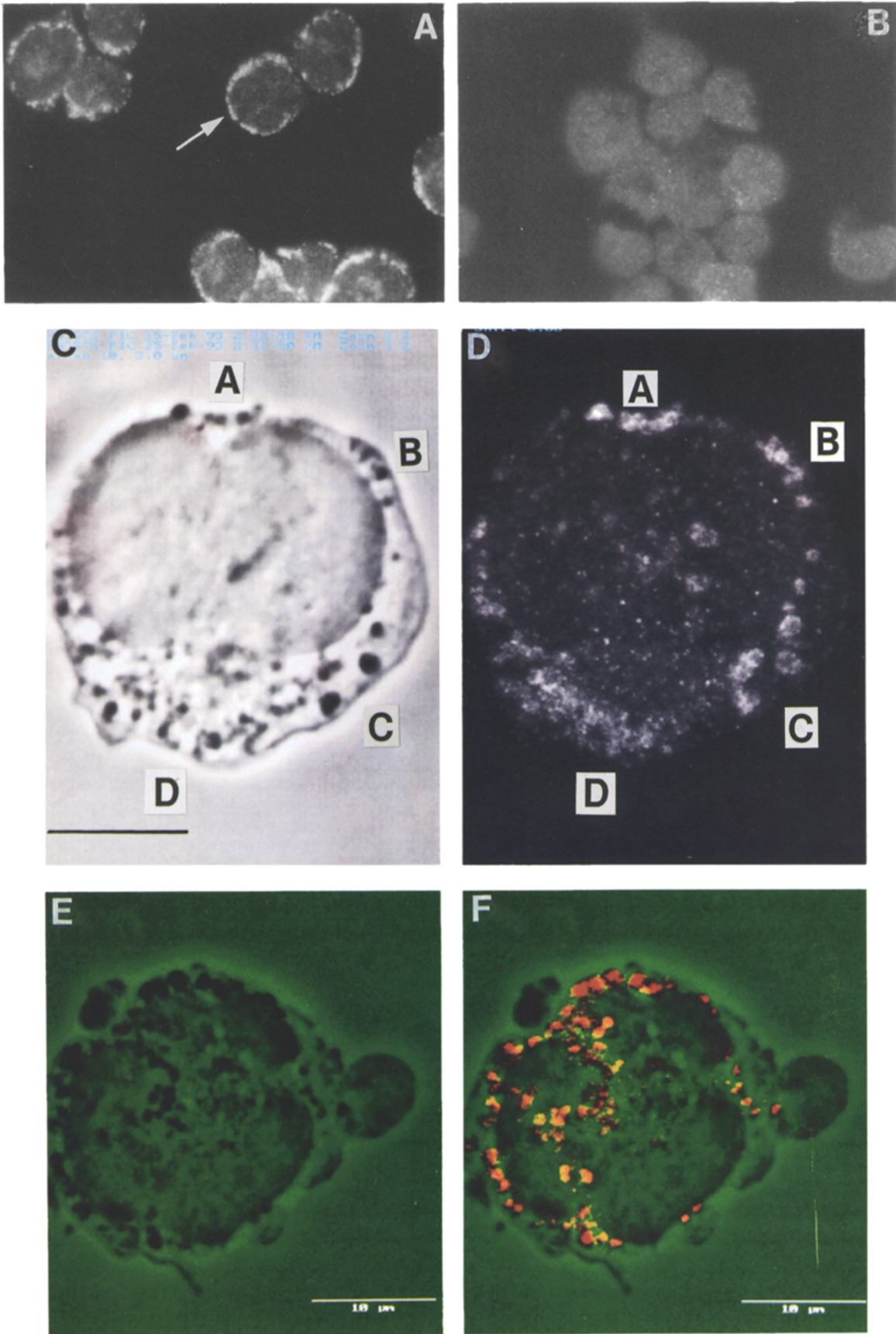


Figure 2. Immunofluorescent staining for the mcl-1 protein is prominent in punctate, cytoplasmic organelles that accumulate Rhodamine123. ML-1 cells were incubated with TPA (as in Fig. 1) to induce expression of the mcl-1 protein. (A and B) Immunofluorescent staining with

PMSF, 12.5 $\mu\text{g/ml}$ aprotinin, 12.5 $\mu\text{g/ml}$ leupeptin, 6.25 $\mu\text{g/ml}$ pepstatin A, 1 mM iodoacetamide, and 0.025% NaN_3 . Lysates were precleared using normal rabbit serum, followed by *Staphylococcus aureus* Cowan I (Boehringer Mannheim Biochemicals, Indianapolis, IN). All steps were carried out at 4°C. The cleared lysates were incubated with antiserum (or preimmune serum) for 1 h, followed by protein A-Agarose for 1 h. After two washes with dilution buffer (50 mM Tris-Cl, pH 7.6, 150 mM NaCl, 0.1% bovine hemoglobin, 1% NP-40, 0.5% deoxycholate, 0.1% SDS, 1 mM EDTA, and 0.025% NaN_3), one wash with TSA (10 mM Tris, pH 8, 140 mM NaCl, and 0.025% NaN_3), and one washed with 50 mM Tris-Cl, pH 6.8, 2 \times SDS sample buffer was added, and the samples were boiled for 5 min, centrifuged, and the supernatant was subjected to SDS-PAGE (15%). After electrophoresis, the gel was fixed in 30% methanol/10% acetic acid for 1 h, treated with ENHANCE (Du Pont Pharmaceuticals, Wilmington, DE), dried, and exposed to x-ray film.

For pulse-chase metabolic labeling, cells were incubated (pulse) with L-[^{35}S]methionine for 3 h, as above. They were then washed twice with methionine-free RPMI 1640 medium and resuspended (chase) at 3×10^5 cells/ml in RPMI 1640 medium containing three times the standard concentration of methionine.

In Vitro Transcription and Translation

A plasmid containing the mcl-1 coding sequence (p3.2; reference 26) was linearized at the 3' end of the cDNA insert and used in *in vitro* transcription with T3 or T7 RNA polymerase. Translation was carried out using a rabbit reticulocyte lysate system (Novagen, Inc., Madison, WI) in the presence or absence of canine pancreatic microsomal membranes (Promega Corp., Madison, WI), following the manufacturer's instructions.

Results

Prominent Mitochondrial Localization of the mcl-1 Protein

We used immunofluorescence, with the affinity-purified anti-mcl-1 antibody preparation, to assess the intracellular localization of mcl-1 in ML-1 cells. Upon exposure to TPA for 3–4 h, ML-1 cells express high levels of mcl-1 mRNA and are committing to differentiation, but they do not yet manifest phenotypic maturation (25, 26). They thus have only a scant cytoplasm, visible as a narrow rim surrounding the nucleus (10). We observed bright, punctate staining for mcl-1 in the cytoplasm of these cells (Fig. 2 A). The specificity of this staining was demonstrated by its inhibition upon addition of excess mcl-1-GST protein (Fig. 2 B), but not GST. Diffuse staining was also seen in the nucleus, but this was not as bright as the cytoplasmic staining, and it was not specifically inhibited by mcl-1-GST (Fig. 2, A and B). As compared to TPA-induced cells, much lower levels of mcl-1 were present in uninduced cells (data not shown), consistent with their lower levels of mcl-1 mRNA (26).

To better visualize the localization of the mcl-1 protein, we viewed TPA-induced ML-1 cells by confocal microscopy. We found the specific staining for mcl-1 (Fig. 2 D) to colocalize with dark cytoplasmic organelles (Fig. 2 C). The mcl-1 protein appeared to surround these organelles, resulting in a roughly spherical, often hollow, appearance (e.g., Fig. 2 D,

above the label C). These organelles accumulated the mitochondrial dye, Rhodamine123 (Fig. 2, E and F).

To confirm the mitochondrial localization of mcl-1, we used two-color staining using the above anti-mcl-1 antibody preparation along with antibodies known to stain mitochondria (AB10A5, or the SPA825 antibody to grp75 [30]). The pattern of staining observed with the anti-mcl-1 antibody (Fig. 3, A and C) was essentially identical to that obtained with the mitochondria-specific antibodies (Fig. 3, B and D). In contrast, a dramatic difference was seen upon two-color staining with the antibody to mcl-1 and antibody to CD63 (data not shown), which stains primarily lysosomes in myeloid cells (1). A difference was also seen upon staining with anti-mcl-1 and an antibody that stains endoplasmic reticulum (SPA827 antibody to immunoglobulin heavy chain binding protein [BiP]; reference 34), the latter yielding a fine, reticular pattern very different from the coarse granular pattern of mcl-1 (data not shown). As a whole, the experiments above demonstrated that mcl-1 was present in the cytoplasm, localizing prominently to mitochondria; they thus provided an initial parallel between the localization of mcl-1 and that of bcl-2.

Membrane Association of the mcl-1 Protein

To test for membrane association of mcl-1, we used Triton X-114 extraction and phase separation. This procedure separates integral membrane proteins from soluble proteins (5). In ML-1 cells exposed to TPA for short times (3–4 h), we detected mcl-1 as a doublet (Fig. 4 A, bands of 42 and 40 kD, which are termed the upper and middle bands because of the detection of an additional lower band at later time points [see below and Fig. 6]). mcl-1 was present in the phase containing the membrane proteins (Fig. 4 A, lane 8, *memb.*), but not in the phase containing the soluble proteins (Fig. 4 A, lane 6, *aq*). mcl-1 was detected using immune (Fig. 4 A, lane 8), but not preimmune (Fig. 4 A, lane 7) serum. As expected, mcl-1 was detected at higher levels in TPA-induced cells (Fig. 4 A, lane 8) as compared to uninduced cells (Fig. 4 A, lane 4). These experiments demonstrated that mcl-1 is a membrane-associated protein, providing a further parallel to bcl-2.

We also studied the membrane association of mcl-1 upon transient transfection into cos-1 cells. We compared a vector containing wild-type mcl-1 (pSG5mcl-1) with a vector lacking a hydrophobic carboxyl terminus (pSG5mcl-1 Δ C27). We found the wild-type pSG5mcl-1 to be predominantly a membrane-associated protein (90%; Fig. 4 B, lanes 7 vs 8); the endogenous mcl-1 in cos-1 cells was also faintly detectable in the membrane fraction (Fig. 4 B, lanes 1 and 3). In contrast, pSG5mcl-1 Δ C27 was predominantly in the aqueous fraction (96%; Fig. 4 B, lane 6). Thus, as in bcl-2 (7, 35, 38), a hydrophobic domain at the carboxyl terminus appears important for the membrane association of mcl-1.

the anti-mcl-1 antibody. The antibody was preincubated with bacterially produced GST protein in A. (GST did not cause any change as compared to no-GST controls [not shown]). The antibody was blocked by preincubation with bacterially produced mcl-1-GST protein in B. The arrow indicates the bright, punctate, cytoplasmic staining that represents mcl-1. (C and D) Confocal microscopy of the immunofluorescent staining for mcl-1. mcl-1 immunofluorescence is in D and the corresponding phase contrast image is in C. The correspondence between mcl-1 and dark cytoplasmic organelles is indicated by the letters at the periphery of the cell. (E and F) Accumulation of the mitochondrial dye, Rhodamine123. Dye accumulation is in F, and the corresponding phase contrast image is in E. The bars on the figures correspond to 10 μm .

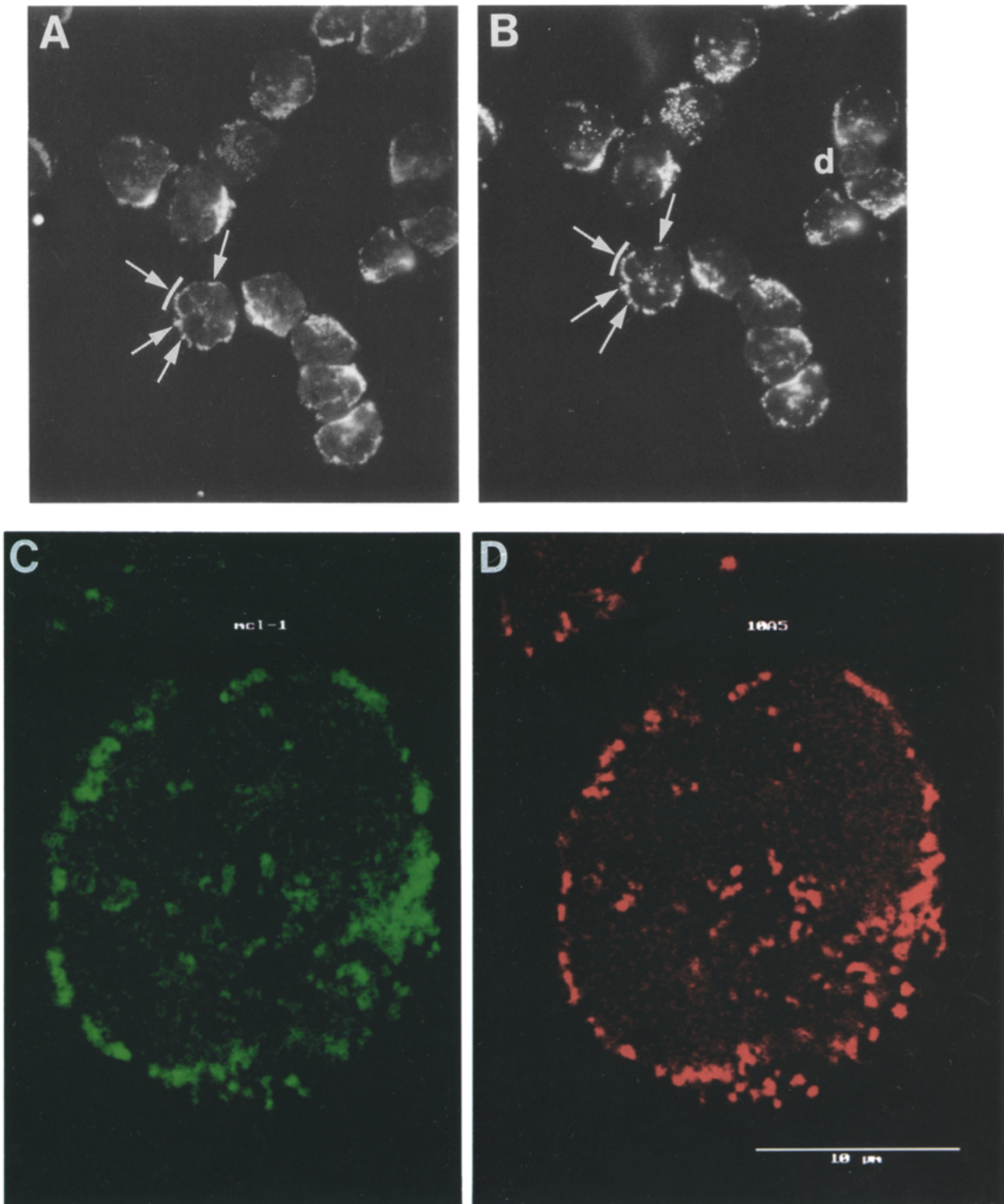


Figure 3. Immunofluorescent staining for *mcl-1* colocalizes with mitochondrial markers. ML-1 cells were exposed to TPA (as in Fig. 1, except that TPA was applied at 8.3×10^{-10} M for 4 h). (*A* and *B*) Cells were stained using both the antibody to *mcl-1* (*A*) and the SPA825 antibody to mitochondrial *grp75* (*B*). Detection of *mcl-1* was with FITC-conjugated goat anti-rabbit IgG and that of *grp75* was with Texas red-conjugated goat anti-mouse IgG. Arrows point out regions of correspondence on a representative cell. A small fraction of TPA-induced ML-1 cells undergo cell death instead of differentiation (9); these cells (*d*) contained lower levels of *mcl-1* than the majority of the differentiating cell population. (*C* and *D*) Cells were stained using both the antibody to *mcl-1* (*C*) and the Ab10A5 antibody that recognizes mitochondria (*D*). The methods used were similar to those in *A* and *B*, except that visualization was by confocal rather than conventional microscopy. Bar, 10 μ m.

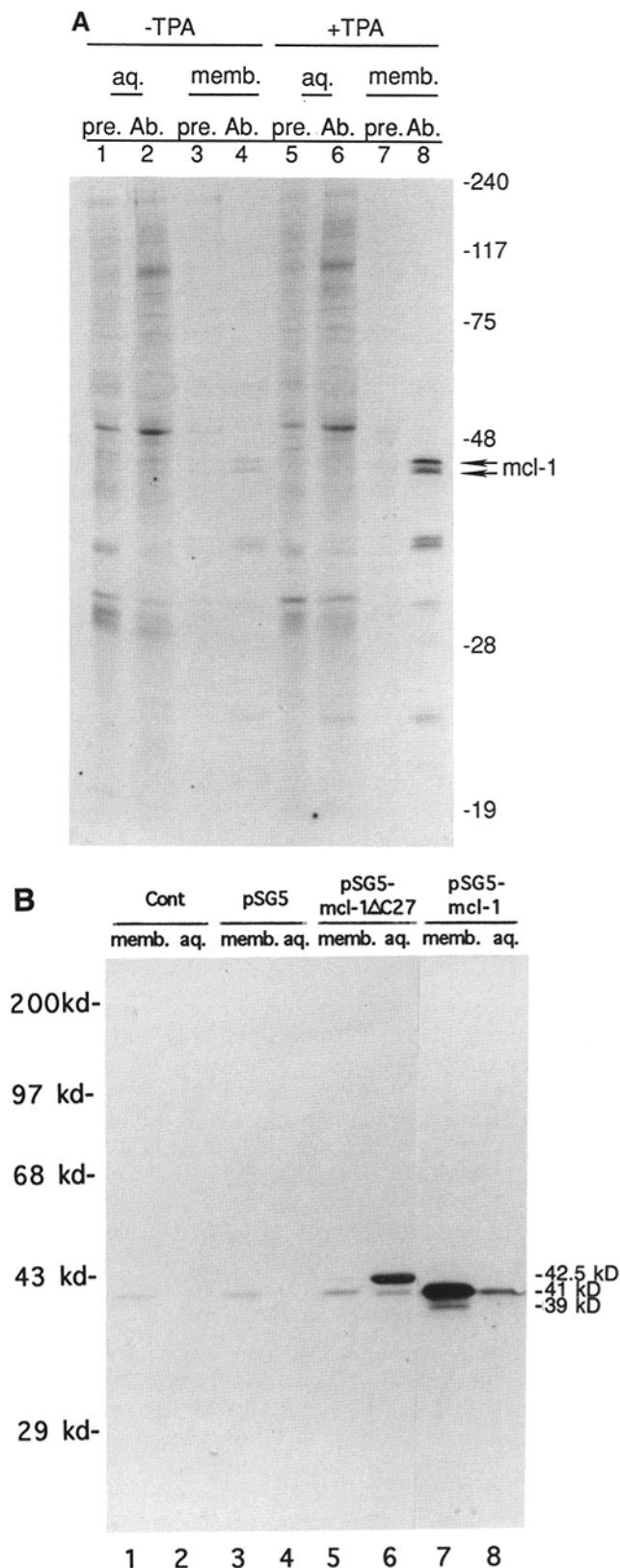


Figure 4. The mcl-1 protein associates with membranes through the hydrophobic carboxyl terminus. (A) ML-1 cells were incubated in the absence (lanes 1-4) or presence (lanes 5-8) of TPA (as in Fig. 1, except that TPA was applied at 1.7×10^{-9} M). Soluble (aq.) and membrane (memb.) proteins were separated using Triton X-114. Aliquots of each phase were subjected to immunoprecipitation using either preimmune serum (pre.) or anti-mcl-1 serum

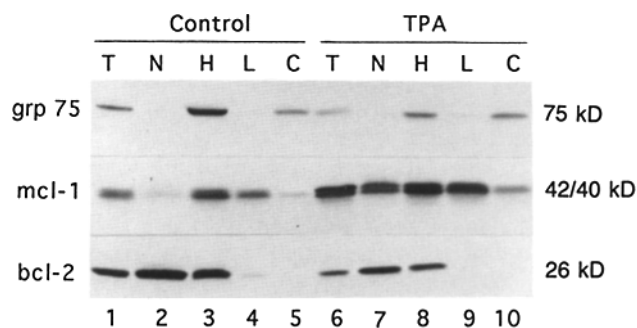


Figure 5. The mcl-1 and bcl-2 proteins exhibit overlapping distributions upon fractionation of ML-1 cells by differential centrifugation. ML-1 cells were incubated in the absence (Control) or presence of TPA (10^{-9} M for 4 h), and they were subjected to differential centrifugation. An aliquot (100 μ g protein) of each fraction, or of the total initial cell lysate (T), was assayed for the presence of mcl-1, bcl-2, and the grp75 mitochondrial protein using Western blotting. The fractions are labeled as follows: N, nuclear; H, heavy membrane; L, light membrane; C, cytosolic. Recovery of protein in the combined fractions (N+H+L+C) was 80-100%. Of the protein recovered, 8-12% was in N, ~19% in H, 17-21% in L, and ~52% in C, with little difference between Control and TPA-induced cells. Cell equivalents loaded per lane ($\times 10^6$) were 1.1, 15.7, 7.0, 6.4, 2.6, 1.1, 16.7, 9.3, 10.7, and 3.5 for lanes 1-10, respectively. The percentage of mcl-1 recovered in the N, H, L, and C fractions from untreated (Control) cells was estimated to be 3%, 54%, 30%, and 13%, respectively. The mcl-1 in the cytosolic fraction (C) is thought to represent protein released into this fraction during homogenization since some grp75 was also found there (lanes 5 and 10). The percentage of bcl-2 recovered in the N, H, and L fractions from untreated (Control) cells was estimated to be 44%, 55%, and 1%, respectively.

Differential Distribution of the mcl-1 and bcl-2 Proteins upon Subcellular Fractionation

We were unable to find satisfactory conditions for staining simultaneously for mcl-1 and bcl-2, although we were able to carry out simultaneous immunofluorescent staining for mcl-1 and various mitochondrial markers (Fig. 3). Therefore, we fractionated ML-1 cells and monitored mcl-1 and bcl-2 by Western blotting. When immature ML-1 cells were fractionated by differential centrifugation, mcl-1 and bcl-2 were both present in the heavy membrane fraction (Fig. 5, Control, lane 3), which contained most of the grp75 (SPA825) mitochondrial marker. This accorded with the mitochondrial staining seen upon immunofluorescence microscopy (Figs. 2 and 3). mcl-1, like bcl-2, was present in other

(Ab.). Arrows indicate the upper and middle mcl-1 protein bands. The doublet of lower molecular mass (~ 35 - 36 kD, lane 8) represents a small amount of degradation of mcl-1 that can occur during the Triton X-114 procedure. (B) Cos-1 cells were transfected with pSG5-mcl-1 or pSG5mcl-1 Δ C27, which does not contain a hydrophobic stretch at the carboxyl terminus. Parallel cultures were not transfected (Cont., lanes 1 and 2), or they were transfected with pSG5 vector alone (no insert, lanes 3 and 4). The membrane association of mcl-1 was assessed as in A, except that detection was by Western blot instead of immunoprecipitation. pSG5mcl-1 Δ C27 was constructed to have the same molecular weight as the wild-type protein, although it proved to migrate slightly more slowly on polyacrylamide gel electrophoresis (see reference 2 and references therein).

fractions in addition to the heavy membrane fraction. However, *mcl-1* differed from *bcl-2* in relative distribution among these fractions. For example, in addition to both being in the heavy membrane fraction in immature cells, *mcl-1* was prominent in the light membrane fraction (30% of total *mcl-1*; Fig. 5, lane 4), where *bcl-2* was barely detectable, while *bcl-2* was prominent in the nuclear fraction (44% of total *bcl-2* similar to previous reports [27]; Fig. 5, lane 2) where *mcl-1* was barely detectable. The nuclear fraction from differential centrifugation can contain contaminating mitochondria (47); this is unlikely to account for the abundance of *bcl-2* there since this fraction did not contain *grp75* (Fig. 5, lane 2). Similarly, the light membrane fraction can contain some small mitochondria (47); this is unlikely to account for the abundance of *mcl-1* there, since this fraction was also devoid of *grp75* (Fig. 5, lane 4). The light membrane fraction can additionally contain disrupted mitochondrial outer membranes (47); this is unlikely to account for the abundance of *mcl-1* relative to *bcl-2* there (Fig. 5, lane 4) since *bcl-2* is an outer membrane protein (27, 35, 38). The light membrane fraction also contains endoplasmic reticulum, Golgi, lysosomes, peroxisomes, ribosomes, and fragments of plasma membrane (47); thus, further work will be necessary to determine which of these components contain *mcl-1*.

When TPA-induced ML-1 cells were subjected to differential centrifugation, *mcl-1* protein was present in all fractions (Fig. 5, TPA, lanes 7-10). When homogenizing TPA-induced cells for differential centrifugation, we were unable to cleanly lyse all cells without causing some nuclear damage (assessed by microscopic inspection). Thus, the results from TPA-induced cells demonstrated a general increase in *mcl-1*, but they could not be used to calculate specific changes in the different fractions. The prominent visualization of *mcl-1* in association with mitochondria (Figs. 2 and 3), together with its presence in additional fractions besides the mitochondria-enriched heavy membrane fraction (Fig. 5), suggest that local *mcl-1* concentrations may be higher at the mitochondrial site than elsewhere. Similarly, *bcl-2* was first localized to mitochondria (21) and was later shown, by high resolution techniques, to also be present elsewhere (27).

Increased Expression of *mcl-1* and Continued Expression of *bcl-2* during ML-1 Cell Differentiation

We followed the time course of expression of the *mcl-1* protein during ML-1 cell differentiation. Total *mcl-1* protein levels increased within 3-6 h of exposure to TPA approximately seven- to nine-fold, respectively; Fig. 6, lanes 3 and 4) after the increase in *mcl-1* mRNA at 1-3 h (26); a decline from this early peak was seen at 24-72 h, although *mcl-1* levels remained above baseline (see 72-h time point, Fig. 6, lane 7). At this time, *bcl-2* levels had decreased (by ~40% on a per-cell basis, as in other similar differentiating systems [11, 21]). We have found the increase in *mcl-1* expression to occur with a more consistent time course than the subsequent decline. Thus, *mcl-1* more closely approached baseline levels at 72 h in some experiments (not shown) than in others (Fig. 6; see also Figs. 1 and 2 in reference 26 for the timing of the decline in the mRNA).

Several closely spaced bands represent the *mcl-1* protein. For example, as shown above (Figs. 1, 4, and 5), *mcl-1* appears as a doublet in Western blots of cells exposed to TPA

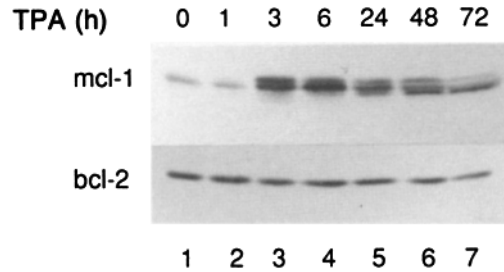


Figure 6. The *mcl-1* and *bcl-2* proteins exhibit distinct but overlapping profiles of expression during TPA-induced ML-1 cell differentiation. ML-1 cells were exposed to 5×10^{-10} M TPA for the indicated times and assayed for the presence of *mcl-1* or *bcl-2* by Western blot. Since a small amount of cell loss accompanies differentiation, the number of viable cell equivalents loaded per lane decreased with time; these values ($\times 10^6$) were 2.1 at 0-3 h, 1.8-1.9 at 6-24 h, and 1.7 at 48-72 h. The fold increase in total *mcl-1*, on a per-cell basis, was ~1, 7, 9, 6, 6, and 4 at 1, 3, 6, 24, 48, and 72 h, respectively. The amount of *bcl-2* per cell remained constant until day 3, when a 40% decrease was noted. At time points of ~24-72 h, a lower *mcl-1* protein band was distinct in addition to the upper and middle *mcl-1* bands. As cells differentiated in response to TPA, the amount of protein (mg) per 10^6 cells increased from 0.12 at 0-3 h, to 0.15 at 6 h, 0.2 at 24 h, 0.26 at 48 h, and 0.32 at 72 h.

for short times (3-4 h; Fig. 6, lane 3 *upper and 24 h middle mcl-1 bands*). In Western blots of untreated cells, the upper band is less prominent (Fig. 6, lane 1). In cells exposed to TPA for longer times (e.g., Fig. 6, lane 5), an additional lower *mcl-1* band becomes evident. This lower band is distinct at 24 h (a very faint band may be seen at earlier times, Fig. 6, lane 4), and it becomes more intense at 48 and 72 h (Fig. 6, lanes 6 and 7). We are currently investigating the differences among the various *mcl-1* bands. The slow time course of appearance of the lower *mcl-1* band suggests that enzymes responsible for the production of this form of *mcl-1* could be present at low levels in untreated cells, and could be induced at part of the differentiation program. Overall, ML-1 cell differentiation was accompanied by an increase in the *mcl-1* protein, followed by a shift from abundance of the upper and middle *mcl-1* bands to the middle and lower bands. This change in expression of *mcl-1* was superimposed upon continued, albeit declining, expression of *bcl-2*.

Lability of the *mcl-1* Protein and Lack of Processing through a Signal Sequence-mediated Mechanism

Because the amino terminus of *mcl-1* has some characteristics of a signal sequence (26), we tested for processing of *mcl-1* through a signal sequence-mediated mechanism. We first translated *mcl-1* mRNA in vitro in the presence of microsomal membranes; the *mcl-1* protein did not undergo cleavage (Fig. 7, lanes 6 and 7). We then tested the protease sensitivity of the products of the in vitro translation reaction; the *mcl-1* protein was not protected from protease digestion (Fig. 7, lanes 8 and 9 vs lanes 6 and 7), showing that *mcl-1* did not undergo translocation across the membranes. This lack of cleavage of the protein and lack of translocation/protease protection indicate that *mcl-1* is not processed by microsomal membranes through a signal sequence-mediated mechanism.

We also used metabolic labeling/immunoprecipitation to

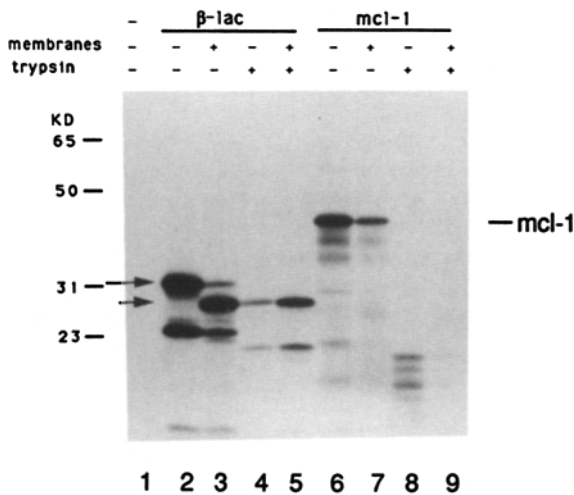


Figure 7. The *mcl-1* protein is not processed through a signal sequence-mediated mechanism. Messenger mRNA representing *mcl-1* (lanes 6–9) or β -lactamase (lanes 2–5) was used in *in vitro* translation in the presence (lanes 3, 5, 7, and 9) or absence (lanes 2, 4, 6, and 8) of pancreatic microsomal membranes. After translation, aliquots of each sample were exposed to trypsin (lanes 4, 5, 8, and 9). When β -lactamase was translated in the presence of membranes, the signal sequence present in the primary translation product was cleaved, yielding a shorter form: The longer form predominated in the absence of membranes (lane 2, *long arrow*), while the shorter form predominated in their presence (lane 3, *short arrow*). This shorter form was protected from trypsin digestion, while the longer form was not (the short form does not disappear in lane 5 [compared to lane 3], while the long form does). A small amount of β -lactamase remained undigested in lane 4. The size of the *mcl-1* *in vitro* translation product was ~ 40 kD. In the presence of membranes, the yield of *mcl-1* was decreased slightly (lane 7).

assess the kinetics of synthesis and degradation of the *mcl-1* protein in ML-1 cells. We found synthesis of the *mcl-1* protein to increase within 2 h of exposure to TPA (~ 2.5 -fold increase in [35 S]methionine incorporation into the upper and middle *mcl-1* bands; Fig. 8 A, lane 7 vs lane 2). Incorporation into the upper band appeared to occur more rapidly than incorporation into the middle band. We did not detect appreciable levels of the lower *mcl-1* band at early time points (1–3 h; Fig. 8 A, lanes 6–8) upon immunoprecipitation, in agreement with results from Western blotting (Fig. 6, lanes 2 and 3). The lower band was detectable upon pulse labeling for 24 h (data not shown), which also agreed with the findings from Western blots (Fig. 6, lane 5). We did not detect secretion of *mcl-1* protein into the medium (Fig. 8 A, lane 5 and 10), consistent with the lack of processing through a signal sequence-mediated mechanism (Fig. 7).

Using pulse-chase, we found turnover of the *mcl-1* protein to occur rapidly in both uninduced and TPA-induced cells (Fig. 8 B, lanes 2–5 and 8–11, respectively). Just as incorporation into the upper band occurred more rapidly (Fig. 8 A), turnover of this band appeared to be somewhat more rapid (Fig. 8 B, half-life of disappearance of ~ 1 h for the upper band, and 2–3 h for the middle band). While a rapid decrease in intensity was seen for both of these bands, an increase was seen in the relative intensity of the middle band as compared to the upper band (Fig. 8 B, lanes 8–10). The more rapid initial appearance of the upper band (Fig. 8 A), as well as its

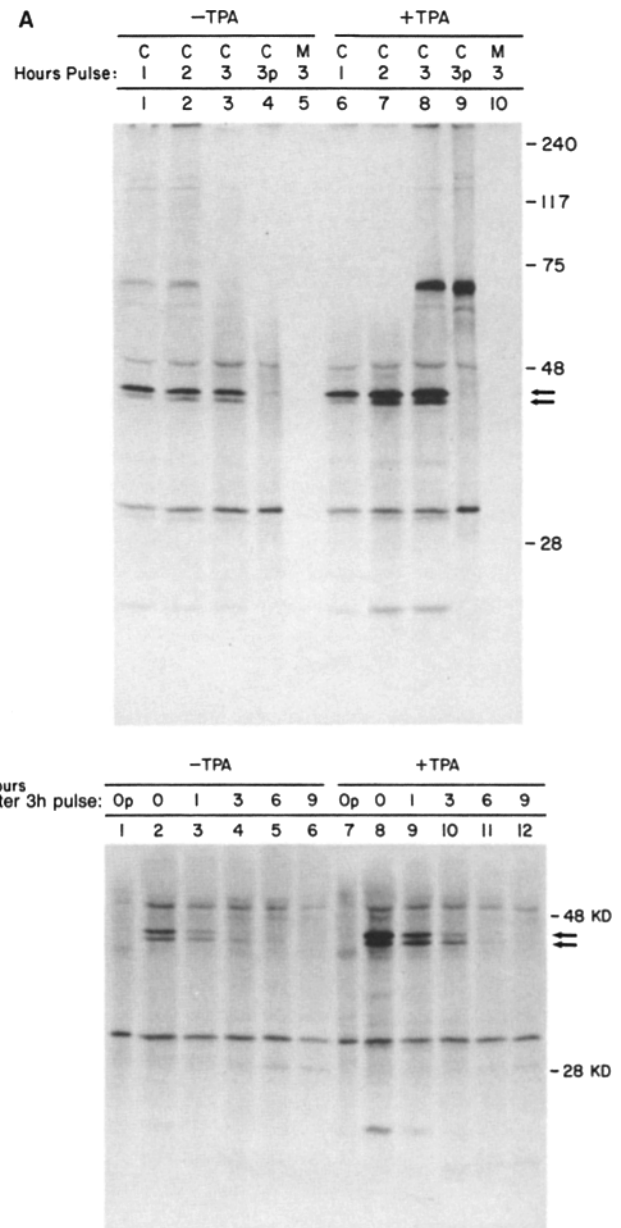


Figure 8. The *mcl-1* protein can be rapidly synthesized and rapidly turned over. (A) ML-1 cells were exposed to [35 S]methionine in the absence (lanes 1–5) or presence (lanes 6–10) of 1.7×10^{-9} M TPA. Immunoprecipitation of cell (C) lysates for *mcl-1* was carried out at 1, 2, and 3 h (5×10^6 cells). The culture medium (M) was assayed at 3 h. Immunoprecipitation using preimmune serum (p; lanes 4 and 9) served as a control. Arrows indicate the upper and middle *mcl-1* protein bands. (B) Cells were subjected to a 3-h pulse exposure to [35 S]methionine as in A, followed by a chase with medium containing excess nonradioactive methionine. Immunoprecipitation was carried out at 0, 1, 3, 6, and 9 h into the chase. As in A, preimmune (p; lanes 1 and 7) was used as a control.

rapid disappearance along with the relative increase in the middle band (Fig. 8 B), suggested that the upper band could be a precursor of the middle band; thus, the middle band could represent a processed form of *mcl-1*, the upper band being chased by conversion to the middle band. At 3 h into the chase, the upper and middle *mcl-1* bands were clearly

discernible, although the lower *mcl-1* band was not (Fig. 8 *B*, lane 10); this is probably related to the fact that the labeled *mcl-1* protein disappears rapidly and to the fact that the lower *mcl-1* band is only faintly discernible at this time point on Western blots (Fig. 6, lane 4). At time points after 3 h of the chase, the *mcl-1* protein had declined to essentially undetectable levels.

Interestingly, we detected a protein of low molecular weight that coimmunoprecipitated with *mcl-1* (22-kD band in Fig. 8 *A*, lane 7 and 8 and *B*, lane 8). In a side-by-side coimmunoprecipitation, the 22-kD band that coimmunoprecipitated with *mcl-1* was identical in size to a band that coimmunoprecipitated with *bcl-2* (data not shown, see references 15 and 40 regarding proteins of this size that immunoprecipitate with *bcl-2*). We are therefore investigating whether this *mcl-1*-associated protein might be *bax* (40), which is of the appropriate size and which has recently been shown to interact with *mcl-1* in the yeast two-hybrid system (44). We did not observe coimmunoprecipitation between *mcl-1* and *bcl-2* (*bcl-2* migrated more slowly than the 22-kD protein, *bcl-2* having an apparent molecular mass of 25–26 kD). Overall, these experiments demonstrate that *mcl-1* can be synthesized rapidly and degraded rapidly, and that *mcl-1* coimmunoprecipitates with a 22-kD protein as does *bcl-2*. The increase in steady-state levels of *mcl-1* seen during the early stages of TPA-induced differentiation (Fig. 6) appears to relate to enhanced synthesis of the protein rather than to inhibition of its degradation (Fig. 8).

Discussion

The members of the *bcl-2* gene family appear to function in the control of cell viability. For example, *bcl-2*, *mcl-1*, *bcl-x*, and *ced9* can enhance viability under conditions that would otherwise produce cell death (3, 4, 14, 16, 20, 21, 23, 39, 42, 53). The question thus arises as to the rationale for the existence of multiple gene products with apparently similar functions. One possibility is that different members of this family might act within different intracellular sites. Different family members might also act within different cell types or within one cell type at different stages of differentiation. Accordingly, different family members might be expected to exhibit nonoverlapping patterns of inter- or intracellular distribution. We have investigated the intracellular localization and pattern of expression of one of the cellular members of the *bcl-2* family, *mcl-1*. In differentiating ML-1 cells, we find that the distribution and expression of *mcl-1* and *bcl-2* overlap, but that they are nonidentical. Thus, the expression of these two *bcl-2* family members with similar function may relate, at least partially, to the differential intracellular distribution of the encoded proteins and to the differential timing of their expression during ML-1 cell differentiation.

mcl-1, like *bcl-2*, exhibits a prominent mitochondrial localization upon visualization by immunofluorescence microscopy. Furthermore, *mcl-1* associates with membranes through its hydrophobic carboxyl tail, as does *bcl-2* (38). However, the distribution of *mcl-1*, as assessed by differential centrifugation, reveals some differences from *bcl-2*: in addition to both being in the heavy membrane fraction in immature ML-1 cells, *mcl-1* is also abundant in the light membrane fraction, and *bcl-2* is also abundant in the nuclear fraction. The biological function underlying the coexpress-

ion of these two *bcl-2* family members may relate to this overlapping but nonidentical pattern of intracellular subcompartmentalization. This is because different members of the *bcl-2* family can interact. For example, *bcl-2* interacts with several proteins, including *bax* (15, 40), and we have observed *mcl-1* to coimmunoprecipitate with a protein of similar size. Such interactions can have a dramatic effect on function. In the case of *bcl-2* and *bax*, heterodimers promote cell viability in contrast to *bax/bax* homodimers which have the opposite effect (56). The intracellular compartmentalization and interactions of all of the various cellular *bcl-2* family members have not yet been fully explored in mammalian systems. Indeed, the breadth of the intracellular distribution of *bcl-2* has been appreciated only recently (27, 33). If overlapping but nonidentical distributions prove to be a common finding, intracellular subcompartmentalization could be an important determinant of the interactions, and thus the net effects, of the members of this family.

In addition to overlapping intracellular distributions, the *mcl-1* and *bcl-2* proteins exhibit overlapping expression during TPA-induced ML-1 cell differentiation. *mcl-1* expression is at a minimum in immature cells, and it increases rapidly in early differentiation. In contrast, *bcl-2* expression is at a maximum in immature cells, and it declines slowly in concert with the completion of the maturation process. Thus, throughout most of differentiation, dramatically increased expression of *mcl-1* is superimposed upon continued expression of *bcl-2*. Both of these gene products have the capacity to inhibit apoptosis, *bcl-2* having been tested in a host of different cell lines, including differentiating systems (13, 16, 18, 29, 39, 50, 53), and *mcl-1* having recently been tested in a defined system in which apoptosis is induced by *c-myc* (42). Future experiments will examine whether coexpression of *mcl-1* and *bcl-2* might allow additive or complementary effects. For example, might the increase in *mcl-1* in ML-1 cells serve to augment the effects of *bcl-2* during the critical period of differentiation-induction? Thus, while *bcl-2* (along with minimum amounts of *mcl-1*) might suffice for the maintenance of viability during continuous proliferative cycling, the transition to differentiation might constitute an additional stress on the mechanisms that maintain cell viability, requiring the supplemental expression of *mcl-1*. A role for *mcl-1* in such critical cell transitions or acute stress would be well served by the fact that *mcl-1* is a labile PEST protein that can be synthesized and degraded rapidly.

In ML-1 cells, expression of both *mcl-1* and *bcl-2* declines, but it does not disappear, as differentiation approaches completion. Maximal levels of these viability-promoting gene products may no longer be necessary when cells reach the fully differentiated, viable, nonproliferative stage. This would be consistent with the hypothesis that increased expression of *mcl-1* is of primary importance when cell viability is threatened, such as under conditions of susceptibility to apoptosis, or when cell fate is being determined, such as during the decision to exit the proliferation cycle and initiate differentiation.

Note added in proof. As this article was being reviewed, *bcl-x* was reported to also localize to mitochondria (González-García, M., R. Pérez-Baltestero, L. Ding, L. Duan, L. H. Boise, C. B. Thompson, and G. Nuñez. 1994. *bcl-x_L* is the major *bcl-x* mRNA form expressed during murine development and its product localizes to the mitochondria. *Development (Camb.)* 120:3033.

We thank Dr. James Hildreth, Dr. Chi Dang, and Dr. Daniel Raben for their generous help throughout all phases of this project. We thank Dr. Lan Bo Chen for providing the AB10A5 antibody, and Drs. Alan Eastman and Suzanne Conzen for critical help in writing the manuscript.

This work was supported by National Institutes of Health (NIH) grant CA57359; cDNAs used in this work were isolated with the support of NIH grant CA54385.

Received for publication 26 September 1994 and in revised form 28 November 1994.

References

- Azorsa, D. O., J. A. Hymann, and J. E. Hildreth. 1991. CD63/Pltgp40: a platelet activation antigen identical to the stage-specific melanoma-associated antigen ME491. *Blood*. 78:280-284.
- Bantia, S., W. R. Bell, and C. V. Dang. 1990. Polymerization defect of fibrinogen Baltimore III due to a gamma Asn308→Ile mutation. *Blood*. 75:1659-1663.
- Bissonnette, R. P., F. Echeverri, A. Mahboubi, and D. R. Green. 1992. Apoptotic cell death induced by c-myc is inhibited by bcl-2. *Nature (Lond.)*. 359:552-554.
- Boise, L. H., M. Gonzalez-Garcia, C. E. Postema, L. Ding, T. Lindsten, L. Turka, X. Mao, G. Nunez, and C. B. Thompson. 1993. bcl-x, a bcl-2-related gene that functions as a dominant regulator of apoptotic cell death. *Cell*. 74:597-608.
- Bordier, C. 1981. Phase separation of integral membrane proteins in Triton X-114 solution. *J. Biol. Chem.* 256:1604-1607.
- Borner, C., I. Martinou, C. Mattman, M. Irmeler, E. Schaefer, J.-C. Martinou, and J. Tschopp. 1994. The protein bcl-2alpha does not require membrane attachment, but two conserved domains to suppress apoptosis. *J. Cell Biol.* 126:1059-1068.
- Chen-Lyvy, Z., and M. L. Cleary. 1990. Membrane topology of the Bcl-2 proto-oncogenic protein demonstrated in vitro. *J. Biol. Chem.* 265:4929-4933.
- Cleary, M. L., S. D. Smith, and J. Sklar. 1986. Cloning and structural analysis of cDNA for bcl-2 and a hybrid bcl-2/immunoglobulin transcript resulting from the t(14;18) translocation. *Cell*. 47:19-28.
- Craig, R. W., O. S. Frankfurt, H. Sakagami, K. Takeda, and A. Bloch. 1984. Macromolecular and cell cycle effects of different classes of agents inducing the maturation of human myeloblastic leukemia (ML-1) cells. *Cancer Res.* 44:2421-2429.
- Craig, R. W., and H. L. Buchan. 1989. Differentiation-inducing and cytotoxic effects of tumor necrosis factor and interferon-gamma in myeloblastic ML-1 cells. *J. Cell Physiol.* 141:46-52.
- Craig, R. W., H. L. Buchan, C. I. Civin, and M. B. Kastan. 1993. Altered cytoplasmic/nuclear distribution of the c-myc protein in differentiating ML-1 human myeloid leukemia cells. *Cell Growth & Dev.* 4:349-357.
- Delia, D., A. Aiello, D. Soligo, E. Fontanella, C. Melani, F. Pezzella, M. A. Pierotti, and G. D. Porta. 1992. bcl-2 protooncogene expression in normal and neoplastic human myeloid cells. *Blood*. 79:1291-1298.
- Fairbairn, L. J., G. J. Cowling, B. M. Reipert, and T. M. Dexter. 1993. Suppression of apoptosis allows differentiation and development of a multipotent hemopoietic cell line in the absence of added growth factors. *Cell*. 74:823-832.
- Fanidi, A., E. A. Harrington, and G. I. Evan. 1992. Cooperative interaction between c-myc and bcl-2 proto-oncogenes. *Nature (Lond.)*. 359:554-556.
- Fernandez-Sarabia, M. J., and J. R. Bischoff. 1993. Bcl-2 associates with the ras-related protein R-ras p23. *Nature (Lond.)*. 366:274-275.
- Garcia, I., I. Martinou, Y. Tsujimoto, and J. Martinou. 1992. Prevention of programmed cell death of sympathetic neurons by the bcl-2 proto-oncogene. *Science (Wash. DC)*. 258:302-304.
- Gratiot-Deans, J., L. Ding, T. A. Turka, and G. Nunez. 1993. bcl-2 proto-oncogene expression during human T cell development. Evidence for biphasic regulation. *J. Immunol.* 151:83-91.
- Hartley, S. B., M. P. Cooke, D. A. Fulcher, A. W. Harris, S. Corey, A. Basten, and C. C. Goodnow. 1993. Elimination of self-reactive B lymphocytes proceeds in two stages: arrested development and cell death. *Cell*. 72:325-335.
- Henderson, S., D. Huen, M. Rowe, C. Dawson, G. Johnson, and A. Rickinson. 1993. Epstein-Barr virus-encoded BHRF1 protein, a viral homologue of Bcl-2, protects human B cells from programmed cell death. *Proc. Natl. Acad. Sci. USA*. 90:8479-8483.
- Hengartner, M. O., and H. R. Horvitz. 1994. C. elegans cell survival gene ced-9 encodes a functional homolog of the mammalian proto-oncogene bcl-2. *Cell*. 76:665-676.
- Hockenbery, D., G. Nunez, C. Minniman, R. D. Schreiber, and S. J. Korsmeyer. 1990. Bcl-2 is an inner mitochondrial membrane protein that blocks programmed cell death. *Nature (Lond.)*. 348:334-336.
- Hockenbery, D. M., M. Zutter, W. Hickey, and M. Nahm. 1991. BCL2 protein is topographically restricted in tissues characterized by apoptotic cell death. *Proc. Natl. Acad. Sci. USA*. 88:6961-6965.
- Kamesaki, S., H. Kamesaki, T. J. Jorgensen, A. Tanizawa, Y. Pommier, and J. Cossman. 1993. bcl-2 protein inhibits etoposide-induced apoptosis through its effects on events subsequent to topoisomerase II-induced DNA strand breaks and their repair. *Cancer Res.* 53:4251-4256.
- Kitada, S., T. Miyashita, S. Tanake, and J. C. Reed. 1993. Investigations of antisense oligonucleotides targeted against bcl-2 RNAs. *Antisense Res. & Dev.* 3:157-169.
- Kozopas, K. M., H. L. Buchan, and R. W. Craig. 1990. Improved coupling between proliferation-arrest and differentiation-induction in ML-1 human myeloblastic leukemia cells. *J. Cell Physiol.* 145:575-586.
- Kozopas, K. M., T. Yang, H. L. Buchan, P. Zhou, and R. W. Craig. 1993. MCL1, a gene expressed in programmed myeloid cell differentiation, has sequence similarity to BCL-2. *Proc. Natl. Acad. Sci. USA*. 90:3516-3520.
- Krajewski, K., S. Tanaka, S. Takayama, M. J. Schibler, W. Fenton, and J. C. Reed. 1993. Investigation of the subcellular distribution of the bcl-2 oncoprotein: Residence in the nuclear envelope, endoplasmic reticulum, and outer mitochondrial membranes. *Cancer Res.* 53:4701-4714.
- Lin, E. Y., A. Orlofsky, M. S. Berger, and M. B. Prystowsky. 1993. Characterization of A1, a novel hemopoietic-specific early-response gene with sequence similarity to bcl-2. *J. Immunol.* 151:1979-1988.
- Linette, G. P., M. J. Grusby, S. M. Hedrick, T. H. Hansen, L. H. Glimcher, and S. J. Korsmeyer. 1994. Bcl-2 is upregulated at the CD4*8* stage during positive selection and promotes thymocyte differentiation at several control points. *Immunity*. 1:197-205.
- Manning-Krieg, U. C., P. E. Schjerer, and G. Schatz. 1991. Sequential action of mitochondrial chaperones in protein import into the matrix. *EMBO (Eur. Mol. Biol. Organ.) J.* 10:3273-3280.
- McDonnell, T. J., N. Deane, F. M. Platt, G. Nunez, U. Jaeger, J. P. McKearn, and S. J. Korsmeyer. 1989. bcl-2-immunoglobulin transgenic mice demonstrate extended B cell survival and follicular lymphoproliferation. *Cell*. 57:79-88.
- Merino, R., L. Ding, D. Veis, S. Korsmeyer, and G. Nunez. 1994. Developmental regulation of the Bcl-2 protein and susceptibility to cell death of B lymphocytes. *EMBO (Eur. Mol. Biol. Organ.) J.* 13:683-691.
- Monaghan, P., D. Robertson, T. Andrew, S. Amos, M. J. S. Dyer, D. Y. Mason, and M. F. Greaves. 1992. Ultrastructural localization of BCL-2 protein. *J. Histochem. Cytochem.* 40:1819-1825.
- Munro, S., and H. Pelham. 1986. An Hsp70-like protein in the ER: identity with the 78 kd glucose-regulated protein and immunoglobulin heavy chain binding protein. *Cell*. 46:291-300.
- Nakai, M., A. Takeda, M. L. Cleary, and T. Endo. 1993. The bcl-2 protein is inserted into the outer membrane but not into the inner membrane of rat liver mitochondria in vitro. *Biochem. Biophys. Res. Commun.* 196:233-239.
- Nakayama, K.-I., K. Nakayama, I. Negishi, K. Kuida, Y. Shinkai, M. Louie, L. Fields, P. Lucas, V. Stewart, F. Alt, and D. Loh. 1993. Disappearance of the lymphoid system in bcl-2 homozygous mutant chimeric mice. *Science (Wash. DC)*. 261:1584-1588.
- Neilan, J. G., Z. Lu, C. L. Afonso, G. F. Kutish, M. D. Sussman, and D. L. Rock. 1993. An African swine fever virus with similarity to the proto-oncogene bcl-2 and the Epstein-Barr virus gene BHRF1. *J. Virol.* 67:4391-4394.
- Nguyen, M., D. G. Millar, V. W. Yong, S. J. Korsmeyer, and G. C. Shore. 1993. Targeting of Bcl-2 to the mitochondrial outer membrane by a COOH-terminal signal anchor sequence. *J. Biol. Chem.* 268:25265-25268.
- Nunez, G., L. London, D. Hockenberry, M. Alexander, J. P. McKearn, and S. J. Korsmeyer. 1991. Deregulated Bcl-2 gene expression selectively prolongs survival of growth factor-deprived hemopoietic cell lines. *J. Immunol.* 144:3602-3610.
- Oltvai, Z. N., C. L. Millman, and S. J. Korsmeyer. 1993. Bcl-2 heterodimerizes in vivo with a conserved homolog, bax, that accelerates programmed cell death. *Cell*. 74:609-619.
- Pearson, G. R., J. Luka, L. Petti, J. Sample, M. Birkenback, D. Braun, and E. Kieff. 1987. Identification of an Epstein-Barr virus early gene encoding a second component of the restricted early antigen complex. *Virology*. 160:151-161.
- Reynolds, J. E., T. Yang, L. Qian, J. D. Jenkinson, P. Zhou, A. Eastman, and R. W. Craig. 1994. Mcl-1, a member of the bcl-2 family delays apoptosis induced by c-myc overexpression in Chinese hamster ovary cells. *Cancer Res.* 54:6348-6352.
- Rogers, S., R. Wells, and M. Richsteiner. 1986. Amino acid sequences common to rapidly degraded proteins: the PEST hypothesis. *Science (Wash. DC)*. 234:364-368.
- Sato, T., M. Hanada, S. Bodrug, S. Irie, N. Iwama, L. H. Boise, C. B. Thompson, E. Golemis, L. Fong, H.-G. Wang, and J. C. Reed. 1994. Interactions among members of the Bcl-2 protein family analyzed with a yeast two-hybrid system. *Proc. Natl. Acad. Sci. USA*. 91:9238-9242.
- Seldin, R. F. 1987. Transfection using DEAE-Dextran. In *Current Protocols in Molecular Biology*. F. M. Ausubel, R. Brent, R. E. Kingston, D. D. Moore, J. A. Smith, J. G. Seidman, and K. Struhl, editors. John Wiley & Sons, Inc., New York. 9.2.1-9.2.6.
- Sentman, C., J. Shutter, D. Hockenberry, D. Kanagawa, and S. Korsmeyer. 1991. bcl-2 inhibits multiple forms of apoptosis but not negative selection in thymocytes. *Cell*. 67:879-888.

47. Sheeler, P. 1981. Centrifugal fractionation of tissues and cells: basic approaches and instrumentation. *Centrifugation in Biology and Medical Science*. John Wiley & Sons, Inc., New York. pp. 31-46.
48. Strasser, A., A. Harris, and S. Cory. 1991a. *bcl-2* transgene inhibits T cell death and perturbs thymic self-censorship. *Cell*. 67:889-899.
49. Strasser, A., S. Whittingham, D. Vaux, M. Bath, J. Adams, S. Cory, and A. Harris. 1991b. Enforced BCL2 expression in B- lymphoid cells prolongs antibody responses and elicits autoimmune disease. *Proc. Natl. Acad. Sci. USA*. 88:8661-8665.
50. Strasser, A., A. Harris, L. M. Corcoran, and S. Cory. 1994. Bcl-2 expression promotes B- but not T-lymphoid development in scid mice. *Nature (Lond.)*. 368:457-460.
51. Tanaka, S., K. Saito, and J. C. Reed. 1993. Structure- function analysis of the *bcl-2* oncoprotein. *J. Biol. Chem.* 268:10920-10926.
52. Tsujimoto, Y., and C. M. Croce. 1986. Analysis of the structure, transcripts, and protein products of *bcl*, the gene involved in human follicular lymphoma. *Proc. Natl. Acad. Sci. USA*. 83:5214-5218.
53. Vaux, D. L., S. Cory, and J. M. Adams. 1988. Bcl-2 gene promotes hemopoietic cell survival and cooperates with *c-myc* to immortalize Pre-B cells. *Nature*. 335:440-442.
54. Veis, D., C. Sorenson, J. Shutter, and S. Korsmeyer. 1993. Bcl-2-deficient mice demonstrate fulminant lymphoid apoptosis, polycystic kidneys, and hypopigmented hair. *Cell*. 75:229-240.
55. Veis, D. J., C. L. Sentman, E. A. Bach, and S. J. Korsmeyer. 1993. Expression of the Bcl-2 protein in murine and human thymocytes and in peripheral T lymphocytes. *J. Immunol.* 151:2546-2554.
56. Yin, X.-M., Z. Oltvai Z, and S. J. Korsmeyer. 1994. BH1 and BH2 domains of *bcl-2* are required for inhibition of apoptosis and heterodimerization with *bax*. *Nature* 369:321-323.